Australian Government
Department of Defence
Defence Science and
Technology Organisation

# Ab Initio Computational Chemical Studies of Molecular Processes and Decomposition in Ammonium Perchlorate

A. White

DSTO-TR-1552

**Australian Government**
**Department of Defence**
Defence Science and
Technology Organisation

# Ab Initio Computational Chemical Studies of Molecular Processes and Decomposition in Ammonium Perchlorate

*A. White*

**Weapons Systems Division**
Systems Sciences Laboratory

DSTO-TR-1552

**ABSTRACT**

Ammonium perchlorate is widely used as an oxidiser in composite propellants for rocket motors. Its decomposition is of interest in stability, sensitivity and combustion studies for rocket motor safety and performance analysis and prediction. This document presents some theoretical studies conducted to yield insights into the mechanisms and kinetics of ammonium perchlorate decomposition.

**RELEASE LIMITATION**

*Approved for public release*

*Published by*

*DSTO Systems Sciences Laboratory*
*PO Box 1500*
*Edinburgh South Australia 5111 Australia*

*Telephone: (08) 8259 5555*
*Fax: (08) 8259 6567*


*AR- 013-032*
*February 2004*

**APPROVED FOR PUBLIC RELEASE**

# Ab Initio Computational Chemical Studies of Molecular Processes and Decomposition in Ammonium Perchlorate

## Executive Summary

The low-temperature decomposition of solid ammonium perchlorate (AP) is a factor in its sensitivity, compatibility and safety and of propellants containing it. Furthermore, the products resulting from the decomposition can oxidise the binder and adversely affect mechanical and ballistic properties. Consequently, these issues are of importance to the Australian Defence Force (ADF) for the safety and service-life of munitions.

In conjunction with experimental studies, the modelling studies described in this report were conducted to better understand the mechanisms of decomposition in AP. They will also serve as a baseline for similar studies involving new materials such as ammonium dinitramide ($NH_4N(NO_2)_2$, ADN) that are proposed as oxidisers in propellants designed for low signature and low sensitivity.

The proton transfer process was studied in depth as this is thought to be the preferred mechanism for the initial step in AP decomposition. In this process, a proton ($H^+$) is transferred from an ammonium cation to a perchlorate anion to form the neutral species ammonia and perchloric acid. For the proton transfer to occur, a transition state must be passed through which is higher in energy than either the reactants or the products. The energy required to reach this state is known as the activation energy.

Although AP is an ionic crystalline solid, for computational tractability, initial studies modelled the transfer of a proton from a single ammonium cation to a single perchlorate anion (this is often referred to as a "gas phase" reaction, because it is only in the gas phase where it is possible to ignore the interaction of other ions or molecules). These calculations indicated that the activation energy required for proton transfer is very small and, as might be expected, the presence of ions in the gas phase is not favoured and perchloric acid and ammonia is the preferred arrangement.

Later calculations were conducted using a matrix of ions around the ions involved, thus simulating proton transfer in the solid state. The presence of the crystalline matrix was found to inhibit the proton transfer process as the formation of neutral species disrupts the bonding in the crystal. However, crystal relaxation and the migration of the neutral species after proton migration would be expected to lower the activation energy of the decomposition reaction, giving activation energies of the same order as those observed experimentally. Unfortunately, with the computer resources currently available, it was not possible to model these effects. As computational power increases, it is planned to repeat these calculations using more advanced methods.

*This page intentionally left blank*

# Authors

**A. White**
Weapons Systems Division

*Dr Alex White is a Senior Research Scientist in Weapons Propulsion group of Weapons Systems Division, DSTO. He obtained a PhD in 1987 in physical inorganic chemistry studying ligand exchange processes in lanthanide and other complexes. This was followed by a year as a Postdoctoral Fellow at the University of New South Wales, investigating alumina catalyst supports for vehicle emission control. He joined DSTO in 1988 and has since worked in several diverse areas including gun propellant service life, cost-benefit analysis of insensitive munitions and weapons effectiveness studies. His current research interests are computational chemistry, safety and service life of gun and rocket propellants and applications of micro- and nanotechnology.*

*This page intentionally left blank*

# Contents

*This page intentionally left blank*

# 1. Introduction

Conventional solid composite propellants for rocket motors are composed of particles of an oxidiser embedded in a matrix of polymeric binder. Ammonium perchlorate (AP) is widely used as the oxidiser material because it is cheap, contains a large amount of oxygen and, on combustion, converts entirely into gaseous reaction products. Some properties of AP are given in Table 1 [1].

*Table 1. Properties of ammonium perchlorate [1]*

| | |
|---|---|
| formula: | $NH_4ClO_4$ |
| molecular weight: | 117.5 |
| density: | 1.95 g/cm$^3$ |
| energy of formation: | -2414 kJ/kg |
| enthalpy of formation: | -2518 kJ/kg |
| heat of explosion ($H_2O$ liq.): | 2045 kJ/kg |
| oxygen balance: | +34.04 % |
| nitrogen content: | 11.04 % |
| volume of detonation gases: | 803 L/kg |
| decomposition point (deflagrates): | 350 °C |

AP is a crystalline material composed of a network of ammonium cations ($NH_4^+$) and perchlorate anions ($ClO_4^-$). It is stable at room temperature, but decomposes at measurable rates above 150°C [2][1]. In the 1950s, the initial step in the low-temperature (< 300°C) decomposition of AP was believed to be one of the following [3, 4]:

- proton transfer from the ammonium cation to the perchlorate anion to form ammonia ($NH_3$) and perchloric acid ($HClO_4$);
- electron transfer from the perchlorate anion to the ammonium cation; or
- Cl-O bond breakage.

Weight-loss studies found that the activation energy was the same for sublimation and low and high temperature decomposition, being around 125 kJ/mol [5]. This lead to the conclusion that a single, unified, mechanism is responsible for all these processes, believed to be proton transfer, as shown in Figure 1 [5]. However, if the rate of reaction for the high temperature decomposition is followed by pressure measurements, an activation energy of around 160 kJ/mol is obtained.

The explanation for this follows. At both low and high temperatures, the rate-determining step is the proton transfer that occurs in the crystalline AP to form adsorbed ammonia and perchloric acid. At low temperatures, two adsorbed $HClO_4$ molecules can then react to form chlorine oxides, which then oxidise $NH_3$ to form the ultimate products [5, 6, 7]. The rate of decomposition is higher than that of sublimation

[1] However, newer, more accurate methods, such as microcalorimetry, may now enable this decomposition to be measured at much lower temperatures, 50°C or lower.

and any gas phase reactions occurring are not rate-determining, consequently the rate of reaction is determined by the proton transfer with an activation energy of ~125 kJ/mol, whether studied by weight loss or pressure increase.

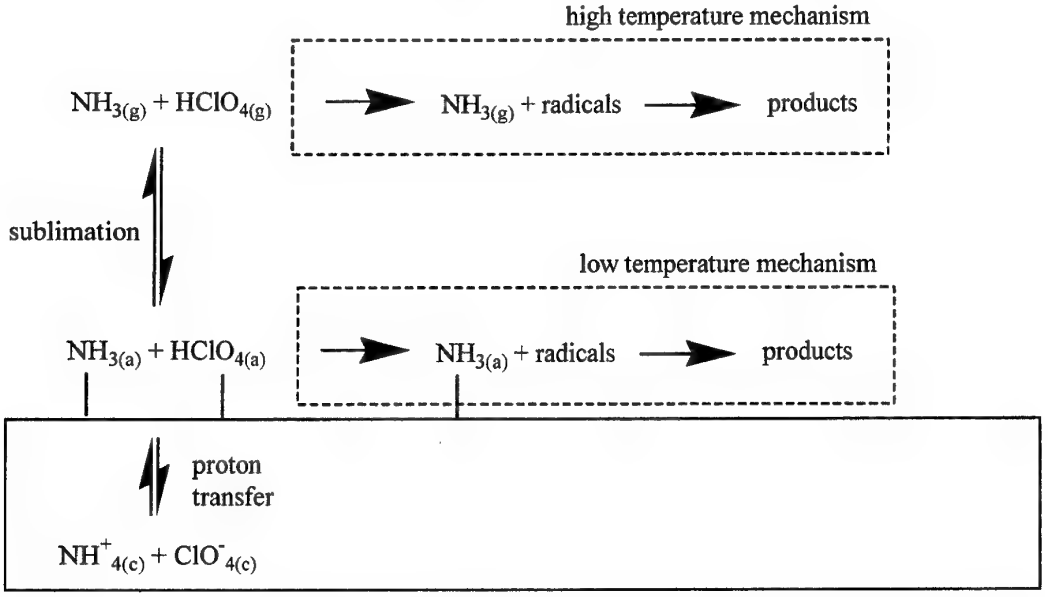


*Figure 1: Proton transfer mechanism [5]*

At higher temperatures, the dissociation products are assumed to sublime before they can decompose on the surface [5, 7]. As the proton transfer is still the rate-determining step for this process, the activation energy measured by weight loss for sublimation is the same as that for the low-temperature decomposition (~125 kJ/mol). However, the activation energy measured by pressure measurements gives the overall activation energy, determined by the rate-determining gas phase reactions (~160 kJ/mol). In both low- and high-temperature decomposition, the ultimate products include $O_2$, $N_2$, $N_2O$, NO, $Cl_2$, $ClO_2$, HCl and $HNO_3$ [2, 3, 7].

The low-temperature decomposition of AP is a factor in the sensitivity, compatibility and safety of this material and propellants containing it. Furthermore, the products resulting from the decomposition can oxidise the binder and adversely affect mechanical and ballistic properties. Consequently, these issues are of importance to the ADF for the safety and service-life of munitions. These modelling studies are being undertaken in conjunction with experimental investigations to illuminate the mechanisms of AP decomposition. They will also serve as a baseline for similar studies involving new materials such as ammonium dinitramide ($NH_4N(NO_2)_2$, ADN), which are proposed as oxidisers in propellants designed for low signature and low sensitivity.

# 2. Results and Discussion

## 2.1 Crystal structures

Crystal structures were obtained from the published crystal parameters (described below) using the Crystal98 suite of programs [8]. Molecular visualisations were generated using HyperChem®. The room-temperature crystal structure of ammonium perchlorate was reported by Smith and Levy [9] to be *Pnma*, a centrosymmetric space group, in accord with earlier studies. Choi, et al. [10] also reported this crystal structure, however, this was disputed by Peyronel and Pignedoli [11], who claimed that the correct structure was the non-centrosymmetric $Pna2_1$ space group. Choi, et al. [12] subsequently refined the structure of AP with the X-ray diffraction data of Peyronel and Pignedoli but found that the structure could still be refined in the space group *Pnma*. Lundgen and Liminga [13] and Lundgren [14] also found that the structure could be refined in the *Pnma* space group. In any case, the differences between the two structures are very small as shown in Figure 2, which shows the crystal structure of ammonium perchlorate refined in the $Pna2_1$ space group [11] and in the *Pnma* space group at 10 K [10, 12, 13, 14].

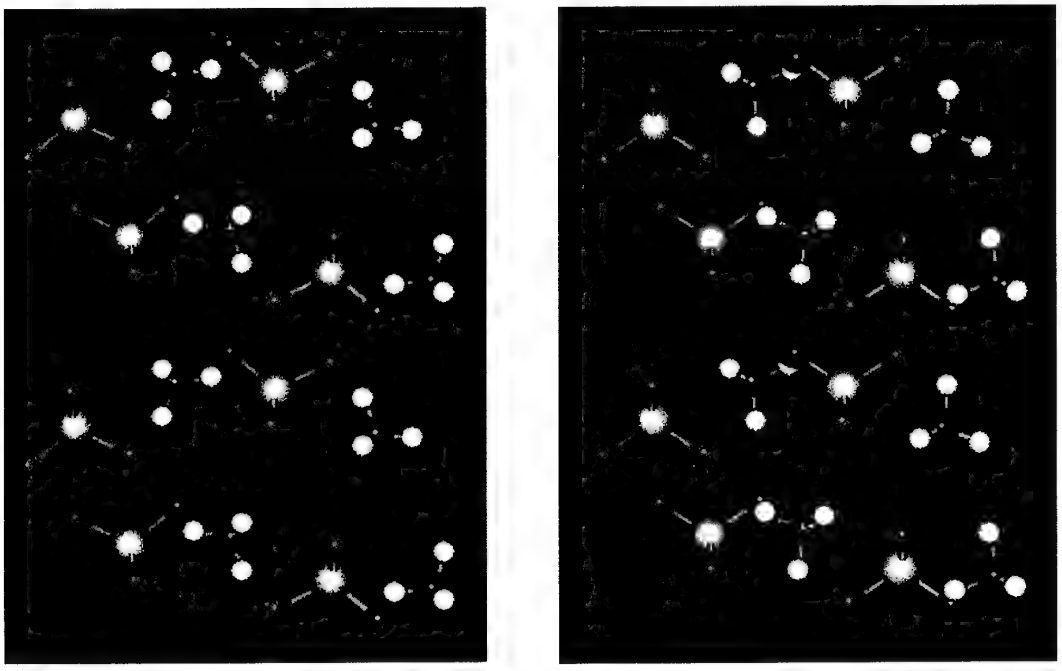

*(a)* *(b)*

*Figure 2: Crystal structures of ammonium perchlorate in (a) the $Pna2_1$ space group [11] and (b) the Pnma space group at 10 K [10, 12, 13, 14] (Chlorine atoms are shown in yellow, nitrogen – blue, oxygen – red and hydrogen – white)*

The main distinction between the $Pna2_1$ and *Pnma* space groups appears to be slight differences in the mean positions of the ammonium groups, which nevertheless undergo complex rotational motions, even at 10 K [9, 10]. As the evidence appears to favour the *Pnma* structure, this will be assumed for the remainder of this paper. In this structure, each ammonium ion is surrounded by 10 oxygen atoms with N-O distances ranging from 2.9 to 3.5 Å [10], as shown in Figure 3.

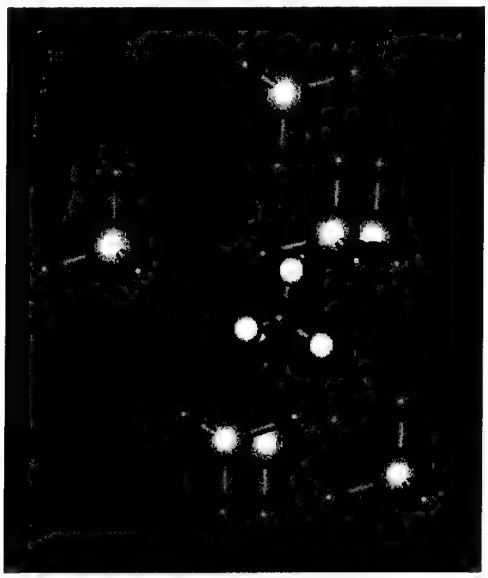

*Figure 3: Ten perchlorate anion oxygens (shown in green) nearest to the ammonium cation in the Pnma structure at 10 K [10]*

## 2.2 B3LYP/6-31G(d) molecular pair studies

Although AP is a solid crystalline material, it is convenient to conduct initial calculations using an isolated pair of molecules or ions. These are sometimes called "gas phase" calculations as it is only in the gas phase where it would be possible to have an isolated pair of molecules or ions interacting. However, as this is unrealistic, the effects of the crystalline matrix will be considered later.

Calculations were performed using a B3LYP method with a 6-31G(d) basis set [15, 16, 17] using the Gaussian 98 package [18] [2]. For energies of optimised structures, a zero-point energy correction was applied, with a scaling factor of 0.9806 from Scott and Radom [20]. This compares with 0.9804 given by Wong [21] and 0.98 given by Bauschlicher and Partridge (0.98) [22].

[2] A general discussion on molecular orbital methods and basis sets may be found in [19].

## 2.2.1 Proton transfer

### *2.2.1.1 Potential energy scan*

In the *Pnma* structure shown in Figure 3, one hydrogen atom of the ammonium ion is pointing directly at one of the oxygen atoms of one of the perchlorate anions, as shown in Figure 4. This hydrogen is atom number 9 (hereinafter called H9) using the numbering scheme also shown in Figure 4. It is connected to the nitrogen (atom number 6 – hereinafter called N6) of the ammonium cation, and is pointing at an oxygen (O4) of the perchlorate anion. The distance between H9 and O4 is 1.93 Å (designated $r_{O4\text{-}H9}$) and the distance from N6 to O4 is 2.95 Å, well within the range of hydrogen bonding.

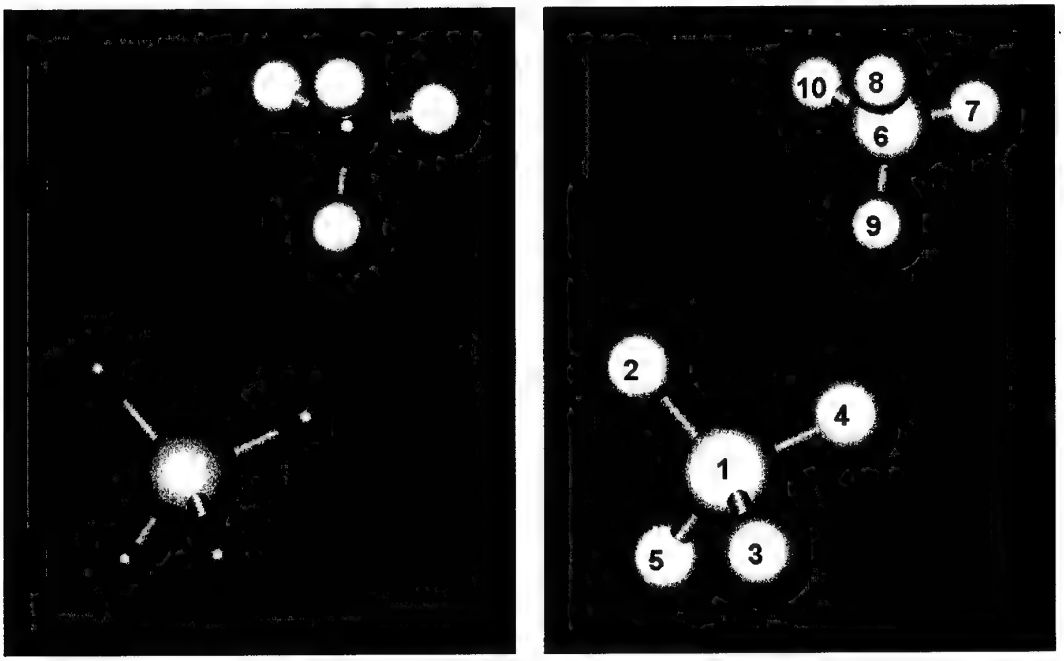


*Figure 4: Ammonium / perchlorate combination in the Pnma crystal structure [10] in which one ammonium hydrogen is pointing directly at one perchlorate oxygen. Also shown is the numbering scheme used to define the atoms.*

This combination gives the closest approach of a hydrogen atom on the ammonium cation to an oxygen atom on the perchlorate anion and appeared to be a good structure to start an examination of the processes involved in the initial phase of the decomposition of AP, in which a hydrogen atom is transferred from an ammonium cation to the perchlorate anion to form ammonia and perchloric acid. As discussed above, this process is thought to occur in the AP crystal matrix, however at this stage these species will be considered in isolation from other molecules or ions, i.e.,

corresponding to a gas phase reaction. The effect of the ammonium perchlorate crystalline matrix on the reaction will be discussed in Section 2.3.

A potential energy scan was undertaken in which the positions of the atoms were held constant in the positions shown in Figure 4, except for H9, which was moved incrementally further from N6 (increasing $r_{N6\text{-}H9}$) and closer to the perchlorate (reducing $r_{O4\text{-}H9}$). The results are shown in Figure 5, which shows the energy relative to the minimum energy with decreasing $r_{O4\text{-}H9}$ [3].

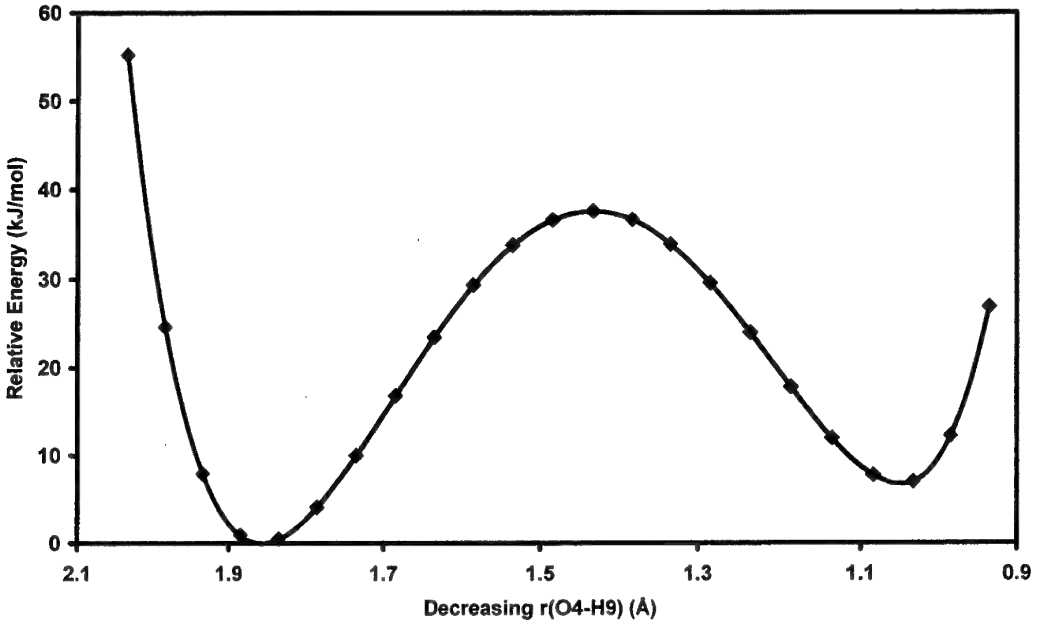


*Figure 5: Variation in energy of the ammonium / perchlorate combination from Figure 4 on moving H9 away from the ammonium ion towards the perchlorate ion*

It can be seen that at the high and low extremes of $r_{O4\text{-}H9}$, the energy rises rapidly as the hydrogen is pushed very close to the nitrogen atom and very close to the oxygen atom respectively, where coulombic repulsion between nuclei predominates. There are two potential energy minima, one at an $r_{O4\text{-}H9}$ distance of about 1.86 Å ($r_{N6\text{-}H9}$ = 1.09 Å), corresponding to the equilibrium N-H bond distance in the $NH_4^+$ / $ClO_4^-$ system and another at $r_{O4\text{-}H9}$ = 1.06 Å ($r_{N6\text{-}H9}$ = 1.89 Å), corresponding to the hydrogen atom having

[3] The reason for defining $r_{O4\text{-}H9}$ and not $r_{N6\text{-}H9}$, although not important in this case, will become apparent later when a relaxed scan is performed on this system. In a relaxed scan, the geometry is allowed to optimise at each step (apart from the bond length being defined). If $r_{N6\text{-}H9}$ is specified and $r_{O4\text{-}H9}$ is allowed to optimise, the calculations can move the ammonium ion around so that H9 (and $r_{N6\text{-}H9}$ being restricted) is not necessarily the hydrogen closest to the perchlorate ion, giving aberrant results.

been transferred to the perchlorate group to give $HClO_4$ and $NH_3$. In between, there is apparently a transition state (potential energy maximum) at an $r_{O4\text{-}H9}$ distance of about 1.43 Å ($r_{N6\text{-}H9}$ = 1.52 Å), giving an activation energy of about 38 kJ/mol. As indicated above, this is lower than that expected for the proton transfer mechanism (~125 kJ/mol) in the crystal. This is not unexpected, as the proton transfer would be expected to be more facile in the gas phase, as other ionic coulombic attractions and hydrogen bonds are not disrupted.

The results obtained from a relaxed potential energy scan on this system are shown in Figure 6. In a relaxed scan, the geometry is allowed to optimise at each step (apart from the bond length being defined). Note that the scale on the y-axis is much smaller than that in Figure 5. The curve is very different to that in Figure 5, with the overall minimum now at an $r_{O4\text{-}H9}$ distance of about 1.06 Å, corresponding to the $NH_3$ / $HClO_4$ system. The $NH_4^+$ / $ClO_4^-$ system has a shallow minimum at about $r_{O4\text{-}H9}$ = 1.68 Å and the activation energy is very small (~1.6 kJ/mol).

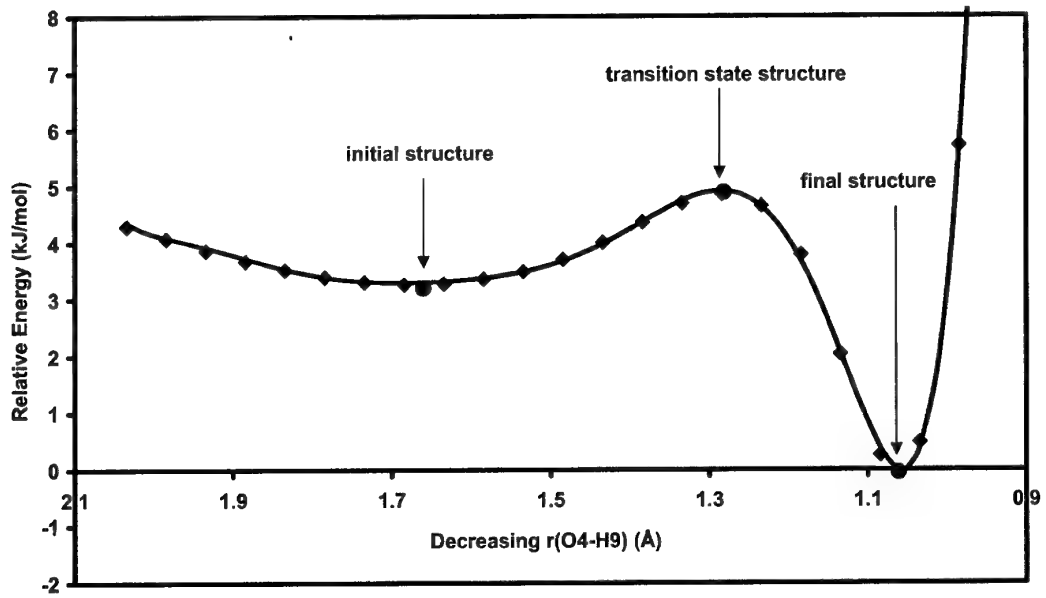


*Figure 6: Variation in energy of the ammonium / perchlorate combination from Figure 4 on moving H9 away from the ammonium ion towards the perchlorate ion allowing the geometry to optimise at each step (except for $r_{O4\text{-}H9}$ which is fixed). As discussed in the next section, also shown (magenta circles) are the energies for unrestricted optimisations of the three structures (i.e. allowing all geometric parameters to optimise, including $r_{O4\text{-}H9}$ ).*

### 2.2.1.2 *Geometry optimisation and transition state structure identification*

Also shown in Figure 6 (as magenta circles) are the energies obtained from unrestricted optimisations on the structures for the three systems, the $NH_4^+$ / $ClO_4^-$ system (the "initial structure"), the $NH_3$ / $HClO_4$ system (the "final structure") and the transition state structure. The optimised structures obtained for these three systems are shown in Figure 7 and selected structural parameters are given in Tables 2 and 3.

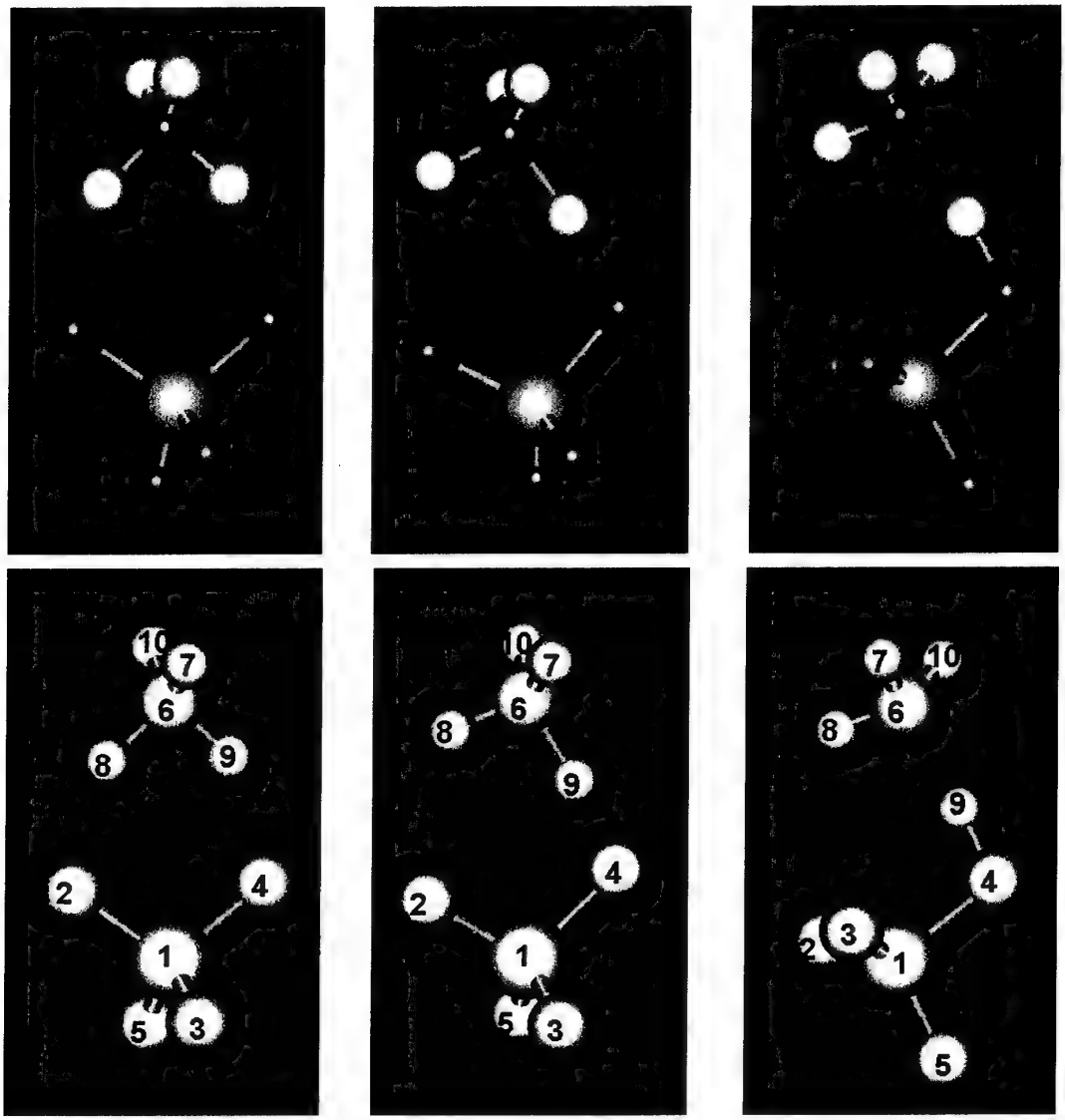


*Figure 7: Optimised structures and numbering schemes for (a) initial, (b) transition and (c) final states*

*Table 2. Selected angles between atoms ("bond angles") of the structures shown in Figure 7*

| Angle | Angle (°) | | |
|---|---|---|---|
| | Initial Structure | Transition State Structure | Final Structure |
| H9-O4-Cl1 | 111.0 | 108.4 | 105.2 |
| H8-O2-Cl1 | 111.3 | 113.4 | 101.6 |
| N6-H9-O4 | 147.3 | 172.7 | 174.9 |
| N6-H8-O2 | 146.2 | 118.6 | 108.0 |
| H8-N6-O4-Cl1 | -4.5 | -3.2 | -30.2 [4] |
| H9-O4-Cl1-O2 | 8.9 | 4.6 | 46.0 |

*Table 3. Selected interatomic distances ("bond lengths") of the structures shown in Figure 7*

| Distance | Interatomic Distance (Å) | | |
|---|---|---|---|
| | Initial Structure | Transition State Structure | Final Structure |
| H9-O4 | 1.66 | 1.28 | 1.06 |
| H9-N6 | 1.07 | 1.23 | 1.57 |
| H8-O2 | 1.67 | 2.17 | 2.73 |
| O2-Cl1 | 1.53 | 1.50 | 1.48 |
| O3-Cl1 | 1.47 | 1.47 | 1.47 |
| O4-Cl1 | 1.54 | 1.59 | 1.64 |
| O5-Cl1 | 1.47 | 1.47 | 1.46 |
| H7-N6 | 1.02 | 1.02 | 1.02 |
| H8-N6 | 1.06 | 1.03 | 1.02 |
| H10-N6 | 1.02 | 1.02 | 1.02 |
| N6-Cl1 | 3.23 | 3.29 | 3.40 |
| N6-O4 | 2.62 | 2.50 | 2.63 |

It can be seen that the initial structure (Fig. 7a) is quite different from that in the *Pnma* crystal structure (Fig 4). In the crystal, the ammonium cation can hydrogen bond with several different perchlorate anions simultaneously; however, in the initial structure, where a single ammonium cation and a single perchlorate anion are isolated, this is not possible. Consequently, the ammonium ion has rotated so that two hydrogen bonds can form between the ions[5]. The transition state structure is very similar to the initial state structure, accounting for their very similar energies (low activation energy). In the final structure, the $NH_3$ and $HClO_4$ have rotated to minimise steric interaction and maximise hydrogen bonding. This is why this structure is lower in energy than the

[4] There is also an alternative structure of the same energy with $d_{H7\text{-}N6\text{-}O4\text{-}Cl1}$ = +30°, i.e. where atoms 3 and 7 are involved in hydrogen bonding instead of atoms 2 and 8.

[5] There is also a structure where three hydrogens of the ammonium are bonded to three oxygen atoms of the perchlorate, however this structure is higher in energy than the initial structure shown in Figure 7a, probably because it brings the nitrogen and chlorine atoms close together. In fact, this structure represents a transition state for the ammonium cation "tumbling" around the perchlorate anion. This is discussed in detail in Section 2.2.2.

initial structure, unlike the structure obtained by simply moving a hydrogen from the ammonium to the perchlorate while maintaining the *Pnma* configuration as shown in Figure 5.

The initial structure has a high degree of symmetry, with the angles $a_{H9\text{-}O4\text{-}Cl1}$ and $a_{H8\text{-}O2\text{-}Cl1}$ essentially equal (Table 2). In addition, the following pairs of bonds are practically equal (Table 3):

- the bond lengths between the ammonium hydrogens and the perchlorate oxygens in the hydrogen bonds, $r_{H9\cdots O4} = 1.66$ Å and $r_{H8\cdots O2} = 1.67$ Å;
- the bond lengths for the N-H part of these hydrogen bonds (i.e., the hydrogens pointing toward the perchlorate anion), $r_{H8\text{-}N6} = 1.06$ Å and $r_{H9\text{-}N6} = 1.07$ Å;
- the N-H bond lengths for the H atoms pointing away from the perchlorate anion, $r_{H7\text{-}N6} = r_{H10\text{-}N6} = 1.02$ Å. These bonds are, as might be expected, slightly shorter than those pointing towards the anion;
- the perchlorate Cl-O bond lengths for the oxygen atoms facing the ammonium cation, $r_{O2\text{-}Cl1} = 1.53$ Å and $r_{O4\text{-}Cl1} = 1.54$ Å; and
- the Cl-O bonds pointing away from the cation, $r_{O3\text{-}Cl1} = r_{O5\text{-}Cl1} = 1.47$ Å. Similarly, slightly shorter than those for the oxygens pointing towards the cation.

In the transition state structure, the ammonium group has rotated clockwise about an axis perpendicular to the page, increasing the angle $a_{N6\text{-}H9\text{-}O4}$ to 172.7°. The dihedral angles $d_{H8\text{-}N6\text{-}O4\text{-}Cl1}$ and $d_{H9\text{-}O4\text{-}Cl1\text{-}O2}$ are practically unchanged, indicating that the ammonium ion has not rotated relative to the O4-Cl1 bond and that the H9-O4 bond has not rotated relative to the rest of the perchlorate ion. The hydrogen bond N6-H8$\cdots$O2 has weakened, increasing the distance between H8 and O2 ($r_{H8\text{-}O2} = 2.17$Å) and decreasing the distance between H8 and N6 ($r_{H8\text{-}N6} = 1.03$Å). On the other hand, the N6-H9$\cdots$O4 hydrogen bond has strengthened, decreasing $r_{H9\text{-}O4}$ to 1.28 Å and increasing $r_{H9\text{-}N6}$ to 1.23Å. The bond lengths for the ammonium hydrogen atoms directed away from the perchlorate anion ($r_{H7\text{-}N6}$ and $r_{H10\text{-}N6}$) and for the perchlorate oxygen atoms directed away from the ammonium cation ($r_{O3\text{-}Cl1}$ and $r_{O5\text{-}Cl1}$) are unchanged.

In the final structure, the hydrogen has completely transferred to the perchlorate to form perchloric acid ($r_{H9\text{-}O4}$ = 1.06Å) and ammonia. The angle $a_{N6\text{-}H9\text{-}O4}$ has further increased to 174.2° and the dihedral angle $d_{H9\text{-}O4\text{-}Cl1\text{-}O2}$ has increased to 46° so that the H9-O4 bond is now staggered in relation to the O2 and O3 oxygen atoms. The dihedral angle $d_{H8\text{-}N6\text{-}O4\text{-}Cl1}$ has also changed as H8 has followed O2 in its rotation. The distance $r_{H8\text{-}O2}$ is too large for significant bonding (confirmed by the fact that $r_{H7\text{-}N6}$, $r_{H8\text{-}N6}$ and $r_{H10\text{-}N6}$ are all identical), so the attraction between H8 and O2 is probably almost purely electrostatic (H8 has a net positive atomic charge of about 0.36e while O2 has a charge of about -0.51e, see the discussion of atomic charges in the following paragraphs). There is, however, still a hydrogen bond N6$\cdots$H9-O4 with $r_{H9\text{-}N6} = 1.57$ Å, keeping the pair of neutral molecules together.

Table 4 shows the atomic charges for the atoms in the structures shown in Figure 7, in conjunction with those for the atoms in the isolated species[6]. In the isolated ions, the ions are totally independent with classical integer charge values for the ions, -1 for $ClO_4^-$ and +1 for $NH_4^+$. On forming the initial structure (the ionic complex $NH_4^+ClO_4^-$ with two hydrogen bonds N6-H8···O2 and N6-H9···O4), the negative charge on the perchlorate anion decreases and the positive charge on the ammonium cation decreases correspondingly as electron density is transferred from the perchlorate to the ammonium. In fact this is a monotonic trend from the isolated ions through the initial, transition state and final structures to the isolated molecules, when finally the charges on the two structures again have classical integer values of zero.

In the isolated ions, the charge distribution is symmetrically distributed among the substituent atoms, as expected. On going to the initial structure, the positive charges on H8 and H9 have increased with the formation of the hydrogen bonds, at the expense of H7 and H10. Similarly, the negative charges on O2 and O4 have increased at the expense of O3 and O5. In the transition state structure, the charge distribution is asymmetric as O4 and H9 are closer together than O2 and H8. In the final structure, after the proton has been transferred and the species rotate to a lower energy configuration, the charges even out somewhat until, in the isolated molecules, the negative charge on the perchloric oxygens and the positive charge on the ammonia hydrogens are distributed fairly evenly (apart from O4 and H9 which are joined, of course).

*Table 4. Atomic charges for atoms in the structures shown in Figure 7 and for atoms in the isolated species*

| atom | Atomic Charge (e) | | | | |
|---|---|---|---|---|---|
| | Isolated Ions | Initial Structure | Transition State Structure | Final Structure | Isolated Molecules |
| totals: | $ClO_4^-$ -1.0<br>$NH_4^+$ 1.0 | $ClO_4^-$ -0.78<br>$NH_4^+$ 0.78 | $ClO_4^-$ -0.74<br>$NH_4^+$ 0.74 | $HClO_4$ -0.12<br>$NH_3$ 0.12 | $HClO_4$ 0.0<br>$NH_3$ 0.0 |
| Cl1 | 1.41 | 1.47 | 1.48 | 1.48 | 1.49 |
| O2 | -0.60 | -0.63 | -0.59 | -0.51 | -0.45 |
| O3 | -0.60 | -0.50 | -0.48 | -0.48 | -0.45 |
| O5 | -0.60 | -0.49 | -0.48 | -0.46 | -0.43 |
| O4 | -0.60 | -0.63 | -0.67 | -0.66 | -0.60 |
| H9 | 0.46 | 0.45 | 0.49 | 0.50 | 0.44 |
| N6 | -0.84 | -0.90 | -0.92 | -0.95 | -0.89 |
| H7 | 0.46 | 0.39 | 0.38 | 0.35 | 0.30 |
| H8 | 0.46 | 0.45 | 0.41 | 0.36 | 0.30 |
| H10 | 0.46 | 0.39 | 0.38 | 0.35 | 0.30 |

[6] Note the ordering of the atoms in the table to put O4 and H9 in the middle of the table as these atoms are connected in the final structure.

In summary, the proton transfer has resulted in the breaking of two weak (i.e., long) hydrogen bonds in the initial structure (H8-O2 and H9-O4) and the formation of a stronger hydrogen bond (H9-N6) and a very strong covalent bond (H9-O4). Thus, it is not surprising that the final structure is lower in energy (albeit only slightly) than the initial structure. The transition state represents an intermediate situation in which one hydrogen bond has been broken (H8-O2) and the H9-O4 hydrogen bond strengthened. However, this strengthening of this bond is not sufficient to entirely compensate for the loss of the other, and the transition state is marginally higher in energy than the initial state.

Now that we have the three fully optimised structures (i.e., stationary points on the potential energy surface), we can obtain more accurate values for their energies and hence for the activation energy. The process requires:

- running an intrinsic reaction coordinate (IRC) calculation to confirm that the transition state is in fact the correct transition state linking the reactants and the products;
- running frequency calculations to obtain scaled zero point energies for each structure; and
- running high-level energy calculations on each of the three structures to obtain more accurate estimates of the energies involved including zero point energies.

#### 2.2.1.3 *Intrinsic reaction coordinate calculation*

An intrinsic reaction coordinate (IRC) calculation was run on the transition state to confirm that it connected the initial and final structures. An IRC calculation starts at the maximum energy point on the potential energy surface corresponding to the transition state and follows the reaction path in both directions, optimising the geometry at each point. In this way, it indicates the reaction initial and final structures and allows confirmation that the transition state is the appropriate one. Some parameters for the three structures discussed above are given in Table 6, along with the final steps in each direction from the IRC calculation.

*Table 5. Selected geometric parameters for the three structures shown in Figure 7 with those for the final steps in each direction from the IRC calculation on the transition state*

| Parameter | Initial Structure | Final step of IRC towards Initial Structure | Transition State Structure | Final step of IRC towards Final Structure | Final Structure |
|---|---|---|---|---|---|
| $r_{H8\text{-}O2}$ (Å) | 1.67 | 2.03 | 2.17 | 2.26 | 2.73 |
| $r_{H8\text{-}N6}$ (Å) | 1.06 | 1.03 | 1.03 | 1.02 | 1.02 |
| $r_{H9\text{-}O4}$ (Å) | 1.66 | 1.41 | 1.28 | 1.11 | 1.06 |
| $r_{H9\text{-}N6}$ (Å) | 1.07 | 1.14 | 1.23 | 1.43 | 1.57 |
| $r_{O2\text{-}C11}$ (Å) | 1.53 | 1.51 | 1.50 | 1.49 | 1.48 |
| $r_{O4\text{-}C11}$ (Å) | 1.54 | 1.57 | 1.59 | 1.63 | 1.65 |
| $a_{H9\text{-}O4\text{-}C11}$ (°) | 111.0 | 109.1 | 108.4 | 107.1 | 105.2 |
| $a_{N6\text{-}H9\text{-}O4}$ (°) | 147.3 | 166.8 | 172.7 | 175.3 | 174.9 |

It can be seen that in almost all cases, the IRC parameters are leading from those of the transition state structure to the initial and final structures, indicating that this transition state is a true transition state between the other two structures. The only exception is the angle $a_{N6\text{-}H9\text{-}O4}$, in which the final step of the IRC calculation towards the final structure is not between those of the transition state structure and the final structure. The discrepancy is minor however, and may arise from inaccuracies in the molecular coordinates from which this parameter is derived.

#### 2.2.1.4 *High accuracy energies*

The energies of the structures are given in Table 6. The total energy at 0 K ($E_0$) is the sum of the electronic energy and the zero point energy. The total energy at 298.15 K (E) is the sum of the electronic and thermal energies (i.e., $E = E_0 + E_{vibrational} + E_{rotational} + E_{translational}$). The enthalpy (H) and free energy (G) have their standard definitions, i.e., $H = E + RT$ and $G = H - TS$ where R is the molar gas constant (8.314 kJ $mol^{-1}$), T is the temperature (298.15 K in this case) and S is the entropy. As RT is the same for all the structures, the relative enthalpies of the transition state and the final structures are the same as their respective relative total energies at 298.15 K.

*Table 6. B3LYP/6-31G(d) energies of the three structures, "initial structure", "transition state structure" and "final structure"*

| Energy | Energy (au) Initial Structure | Transition State Structure | Final Structure |
|---|---|---|---|
| electronic energy | -817.876464 | -817.875820 | -817.877704 |
| zero point energy | 0.063665 | 0.060211 | 0.062361 |
| total energy at 0K | -817.812799 | -817.815609 | -817.815343 |
| total energy at 298.15K | -817.805218 | -817.808426 | -817.807428 |
| enthalpy | -817.804274 | -817.807482 | -817.806484 |
| free energy | -817.845957 | -817.848545 | -817.849089 |
| Energy | Energy relative to Initial Structure (kJ/mol) | | |
| electronic energy | 0.00 | 1.69 | -3.25 |
| zero point energy | 0.00 | -9.07 | -3.42 |
| total energy at 0K | 0.00 | -7.38 | -6.68 |
| total energy at 298.15K | 0.00 | -8.42 | -5.80 |
| enthalpy | 0.00 | -8.42 | -5.80 |
| free energy | 0.00 | -6.79 | -8.22 |

As discussed above, in the uncorrected electronic energies the energy of the transition state is slightly higher than that of the initial state. However once the zero point energy is added, the total energy at 0 K for the transition state structure is apparently lower than either the initial state or the final state. The author suspects that the zero point energy for the Transition State Structure may not be accurate, as it is quite different to both that of the Initial Structure and the Final Structure, but, in any case, the energy differences between the three structures are very small.

#### 2.2.1.5 *Basis set superposition error (BSSE)*

There is one more factor that still has to be considered. The above results are not corrected for basis set superposition error (BSSE). BSSE arises from the fact that as the two species come closer together and interact more, the electrons of each species have more of the other species orbitals available, i.e., the basis set for the transition state is effectively larger than that for the initial and final states, leading to an artificial lowering of the energy (see [19] for a general discussion of basis sets).

The commonly used procedure for correcting for BSSE is called counterpoise correction. This method involves calculating the energy of each individual species in a complex calculated using all basis functions available in the complex by "ghosting" the atoms of the other species in the complex, i.e., retaining the basis functions but setting the atomic number to zero [18]. The energy of the complex is then corrected by subtracting the difference between the energy of the individual species calculated using the basis set of the whole complex and that calculated using only the basis set of the individual species [24]. If we apply the counterpoise correction, the electronic energies relative to the Initial state become 2.25 and -5.69 kJ/mol for the Transition State structure and Final Structure respectively (compared to 1.69 and -3.25 kJ/mol from Table 6). Consequently, the incorporation of BSSE does not significantly affect the above qualitative discussion of the results.

### 2.2.2 Ammonium tumbling

As mentioned above, there is a transition state structure with three hydrogen bonds involving the hydrogens on the ammonium cation and the oxygens on the perchlorate anion. This structure is shown in Figure 8, between two initial structures so that the type of motion occurring is more readily apparent. The initial structure shown in Figure 8(a) is identical to that discussed above (Fig. 7(a)), but has been shown from a different perspective, so as to better illustrate the tumbling process.

In the initial step of the tumbling process, the ammonium rotates about the perchlorate anion, leaving the H9-O4 and H8-O2 bonds intact and forming a new bond between H7 and O3 in the transition state (Fig. 8(b)). The ammonium can then either rotate back to form the original structure, or rotate while keeping the H9-O4 and H7-O3 bonds intact to form an alternative initial structure (Initial Structure', as shown in Figure 8(c)). Alternatively, the ammonium in the transition state could rotate about the perchlorate keeping the H8-O2 and H7-O3 bonds intact to form another alternative initial structure (Initial Structure", not shown). All three initial structures thus formed would be entirely indistinguishable, unless some form of chemical labelling were used, such as substituting one or more of the hydrogen atoms for deuterium atoms or isotopically labelling the oxygens of the perchlorate. Other identical initial structures can be imagined as the ammonium tumbles about the perchlorate. Selected geometric parameters for the structures shown in Figure 8 are given in Tables 7 and 8.

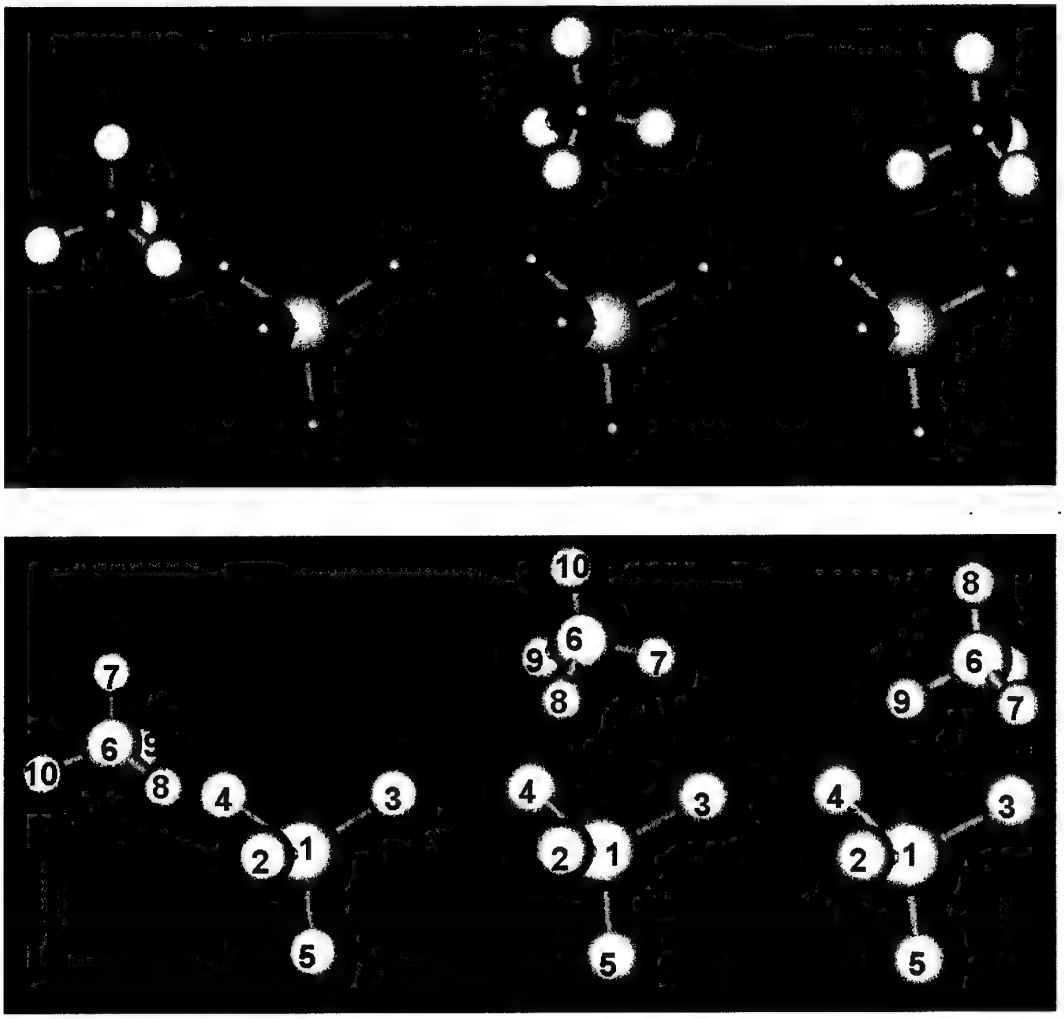


*(a)* *(b)* *(c)*

*Figure 8: Transition state structure (b) for ammonium "tumbling" between two equivalent initial structures (a and c) and the numbering scheme used to indicate the movement of atoms*

The hydrogen bond lengths $r_{H9\text{-}O4}$ and $r_{H8\text{-}O2}$ increase on going from the initial structure to the transition state structure as the number of hydrogen bonds increases from two to three, reducing the electron density available for bonding and increasing the bond lengths. The bond length $r_{H7\text{-}O3}$ decreases, and the bond lengths $r_{H7\text{-}N6}$ and $r_{O3\text{-}Cl1}$ increase as the amount of hydrogen bonding increases on going from Initial Structure to Transition State Structure to Initial Structure'. The other bond lengths do not vary a great deal, except that the nitrogen atom N6 is closer to the chlorine atom Cl1 in the transition state structure, as might be expected.

*Table 7. Selected interatomic distances ("bond lengths") of the structures shown in Figure 8*

| distance | Interatomic Distance (Å) | | |
|---|---|---|---|
| | Initial Structure | Transition State Structure for ammonium tumbling | Initial Structure' (estimated from Initial Structure) |
| H8-O2 | 1.67 | 1.94 | 4.77 |
| H9-O4 | 1.66 | 2.02 | 1.66 |
| H7-O3 | 4.77 | 1.98 | 1.67 |
| N6-Cl1 | 3.23 | 2.92 | 3.23 |
| O2-Cl1 | 1.53 | 1.52 | 1.47 |
| O3-Cl1 | 1.47 | 1.51 | 1.53 |
| O4-Cl1 | 1.54 | 1.51 | 1.54 |
| O5-Cl1 | 1.47 | 1.47 | 1.47 |
| H7-N6 | 1.02 | 1.04 | 1.06 |
| H8-N6 | 1.06 | 1.04 | 1.02 |
| H9-N6 | 1.07 | 1.04 | 1.07 |
| H10-N6 | 1.02 | 1.02 | 1.02 |

*Table 8. Selected angles between three atoms ("bond angles") of the structures shown in Figure 8*

| Angle | Angle (°) | | |
|---|---|---|---|
| | Initial Structure | Transition State Structure for ammonium tumbling | Initial Structure' (estimated from Initial Structure |
| H9-O4-Cl1 | 111.0 | 98.3 | 111.0 |
| H8-O2-Cl1 | 111.3 | 97.8 | 46.9 |
| H7-O3-Cl1 | 56.7 | 98.0 | 111.3 |
| N6-H9-O4 | 147.3 | 125.5 | 147.3 |
| N6-H7-O3 | 62.7 | 128.2 | 146.2 |
| H8-N6-O4-Cl1 | -4.5 | -51.8 | -112.5 |
| H9-O4-Cl1-O2 | 8.9 | 57.3 | 126.9 |

The charges on the atoms are given in Table 9. It can be seen that the major difference in charge distribution on going from Initial Structure to Transition State Structure is an increase in both the negative charge on O3 and the positive charge on N7 as they are brought closer together. Similarly, on going from Transition State Structure to Initial Structure', both the negative charge on O2 and the positive charge on H8 decrease as the distance between them increases.

The transition state for ammonium tumbling has two imaginary frequencies, indicating that it is a second-order saddle point on the potential energy surface (i.e., a point of

maximum energy for two reaction paths). The reaction paths involved can be indicated qualitatively by examination of the normal modes of vibration for these imaginary frequencies. One reaction path gives the transition state structure for the initial structure going to the transition state structure and back to an initial state (ammonium tumbling, as shown in Figure 8). The other appears to be a continuation of the rotation from the initial structure to the transition state structure, bringing one of the hydrogens closer to one of the oxygens, which may be leading to proton transfer and would give a final structure similar to that shown in Figure 7(c). However, as the transition state structure for ammonium tumbling is higher in energy than the one shown in Figure 7(b), the mechanism discussed there for proton transfer would still be preferred.

*Table 9. Atomic charges for atoms shown in Figure 8*

| atom / group | Atomic Charge (e) | | |
|---|---|---|---|
| | Initial Structure | Transition State Structure for ammonium tumbling | Initial Structure' (estimated from Initial Structure) |
| Cl1 | 1.47 | 1.53 | 1.47 |
| O2 | -0.63 | -0.62 | -0.50 |
| O3 | -0.50 | -0.62 | -0.63 |
| O4 | -0.63 | -0.61 | -0.63 |
| O5 | -0.49 | -0.48 | -0.49 |
| ClO4 (total) | -0.78 | -0.80 | -0.78 |
| N6 | -0.90 | -0.90 | -0.90 |
| H7 | 0.39 | 0.43 | 0.45 |
| H8 | 0.45 | 0.44 | 0.39 |
| H9 | 0.45 | 0.43 | 0.45 |
| H10 | 0.39 | 0.40 | 0.39 |
| NH4 (total) | 0.78 | 0.80 | 0.78 |

*Table 10. B3LYP/6-31G(d) energies of the transition state structure for ammonium tumbling compared to the initial structure*

| Energy | Energy of Initial Structure (au) | Energy of Transition State Structure (au) | Energy of Transition State Structure Relative to Initial Structure (kJ/mol) |
|---|---|---|---|
| electronic energy | -817.876464 | -817.874431 | 5.34 |
| zero point energy | 0.063665 | 0.064500 | 2.19 |
| total energy at 0K | -817.812799 | -817.809931 | 7.53 |
| total energy at 298.15K | -817.805218 | -817.803955 | 3.32 |
| enthalpy | -817.804274 | -817.803011 | 3.32 |
| free energy | -817.845957 | -817.839720 | 16.4 |

## 2.3 B3LYP/6-31G(d) studies of proton transfer in the crystalline matrix

The studies presented above consider an ammonium ion and a perchlorate ion in isolation, sometimes referred to as "gas phase" studies. They indicated that there is little difference in energy between all the structures considered and none of the activation energies obtained between initial and transition states are close to those found experimentally for ammonium perchlorate. However, it is believed that the initial stage in the low temperature decomposition of ammonium perchlorate (i.e., the proton transfer from the ammonium ion to the perchlorate ion) occurs in the crystal. Here the ions are surrounded by other ions and there is likely to be a much greater energy penalty involved in disrupting the ionic crystal by effectively replacing two ions in the structure with two neutral molecules.

To study the proton transfer in a crystal structure, an ensemble of ions was considered as shown in Figure 9. The proton transfer occurs between the two ions in the centre of the ensemble, shown in green. The surrounding ions simulate the crystal environment of the two ions in the centre. This ensemble was considered to be the minimum number of ions that could be used to simulate the crystal environment to any degree of accuracy.

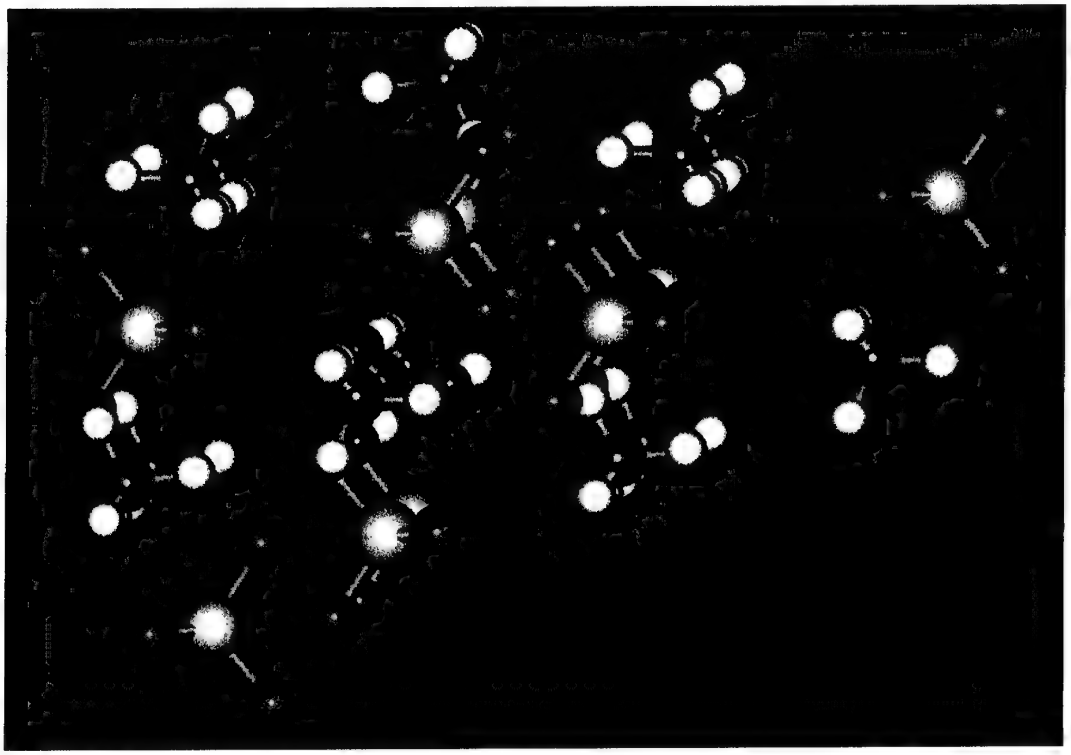

*Figure 9: Ensemble of ammonium ions and perchlorate anions used to simulate the environment encountered in the crystal matrix by the centre ions (shown in green)*

Unfortunately, optimising the geometry of an ensemble such as this is prohibitively expensive in computer time, so energy minima cannot be obtained. Consequently, a scan sequence was used (similar to that shown in Figure 5), moving the proton from the central ammonium ion towards the perchlorate anion. The potential energy curve obtained from such a scan is shown in Figure 10 (shown with decreasing r(O-H) for compatibility with Figures 5 and 6).

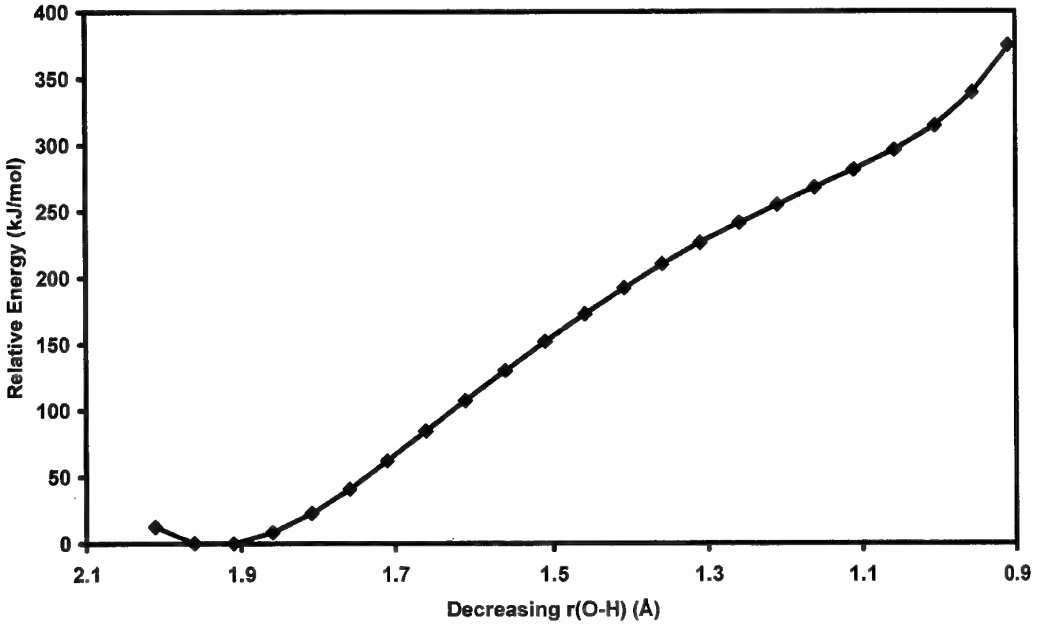


*Figure 10: Variation in energy of the ammonium / perchlorate combination in the crystal ensemble from Figure 9 on moving the hydrogen of the ammonium closest to the perchlorate anion away from the ammonium ion towards the perchlorate ion*

It can be seen that as the proton is progressively removed from the ammonium cation towards the perchlorate anion, the energy of the ensemble rises. This is to be expected, because as mentioned above, the process is creating two neutral molecules, disrupting the ionic matrix. However, superimposed on this energy rise is a curve similar to that shown in Figure 5, with two local minima, one when r(O-H) is between 1.0 and 1.05 (which is also the global minimum where the ions are in their equilibrium positions) and one when r(O-H) is about 1.11 Å, corresponding to the $NH_3/HClO_4$ complex formed in the crystal matrix. The energy required to achieve this state is approximately 300 kJ/mol; between these two minima, is a local maximum corresponding to the transition state. The activation energy required to go from the ground state to the transition state is approximately 180 kJ/mol, which is of the same order as the activation energy experimentally observed for the decomposition of AP, which as discussed in the Introduction above, is about 125 kJ/mol.

It is not surprising that the experimental activation energy is lower than that estimated here as in the real crystal, relaxation in geometry and bonding can occur to compensate for the proton transfer. Also, as mentioned in the Introduction, the products from the proton transfer in the crystal are absorbed on the surface. Thus, it is likely that a synergistic process takes place whereby, as the proton transfer occurs, the geometry and bonding in the remainder of the crystal matrix relaxes and the neutral species migrate to the surface. This would have the effect of lowering the local minimum observed at r(O-H) = 1.11 Å (probably making it a true minimum) and also reducing the activation energy. Unfortunately, at this stage, computations to confirm these suppositions are beyond the computer power currently available to the author.

# 3. Conclusions

Although it was not possible to obtain energies for the various structures involved which gave values which were consistent with those obtained experimentally, the theoretical methods used did yield some interesting insights into the possible behaviours of ammonium perchlorate molecules and ions.

In isolated molecules (gas phase), there are very small energy differences separating the various structures that may be involved in proton transfer mechanisms (Initial Structure, the Transition State Structure and the Final Structure). As might be expected, the presence of ions in the gas phase is not favoured and the Final Structure (i.e., perchloric acid and ammonia) is the preferred arrangement.

Ammonium tumbling around the perchlorate ion (or vice versa) has a very low activation energy and adds another avenue for atomic arrangements that may lead to proton transfer. Basis set superposition error (BSSE) does not appear to affect the results, at least as far as the qualitative discussion is concerned.

The presence of the crystalline matrix, as would be expected, adds a significant amount of resistance to the proton transfer process. However, it was not possible to model the effects of crystal relaxation as neutral species migrate out of the crystal matrix, which would be expected to lower the activation energy.

# 4. References

1. Meyer, R., Explosives (3rd ed.), VCH Verlagsgesellschaft mbH, Weinheim (1987).

2. Jacobs, P.W.M. and Whitehead, H.M., Decomposition and combustion of ammonium perchlorate, *Chem. Rev.*, **69(4)**, 551 - 590 (1969).

3. Bircumshaw, L.L. and Newman, B.H., The thermal decomposition of ammonium perchlorate I. Introduction, experimental, analysis of gaseous products, and thermal decomposition experiments, *Proc. Roy. Soc. (London)*, **A227**, 115-132 (1954).

4. Bircumshaw, L.L. and Newman, B.H., The thermal decomposition of ammonium perchlorate II. The kinetics of the decomposition, the effect of particle size, and discussion of results, *Proc. Roy. Soc. (London)*, **A227**, 228 - 241 (1954).

5. Jacobs, P.W.M. and Russell-Jones, A., On the mechanism of the decomposition of ammonium perchlorate, *AIAA Journal*, **5(4)**, 829 - 830 (1967).

6. Jacobs, P.W.M. and Russell-Jones, A., The thermal decomposition and ignition of mixtures of ammonium perchlorate and copper chromite, *11th Symp. (Intl.) on Combustion*, 457 - 462 (1967).

7. Rosser, W.A.; Inami, S.H. and Wise, H., Thermal decomposition of ammonium perchlorate, *Combustion and Flame*, **12**, 427 - 435 (1968).

8. Saunders, V.R.; Dovesi, R.; Roetti, C.; Causà, M.; Harrison, N.M.; Orlando, R. and Zicovich-Wilson, C.M., Crystal98 User's Manual, University of Torino, Torino (1998).

9. Smith, H.G. and Levy, H.A., Neutron diffraction study of ammonium perchlorate, *Acta Cryst.*, **15**, 1201 - 1204 (1962).

10. Choi, C.S.; Prask, H.J. and Prince, E., Crystal structure of $NH_4ClO_4$ at 298, 78 and 10°K by neutron diffraction, *J. Chem. Phys.*, **61**, 3523 - 3529 (1974).

11. Peyronel, G. and Pignedoli, A., A three-dimensional X-ray redetermination of the crystal structure of ammonium perchlorate, *Acta Cryst.*, **B31**, 2052 - 2056 (1975).

12. Choi, C.S.; Prask, H.J. and Prince, E., Ammonium perchlorate: reinvestigation of the crystal structure at 298 K, *Acta Cryst.*, **B32**, 2919 - 2920 (1976).

13. Lundgren, J.-O. and Liminga, R., X-ray structure of ammonium perchlorate. I. X-ray data collection and estimation of variances of the intensities, *Acta Cryst.*, **B35**, 1023 - 1027 (1976).

14. Lundgren, J.-O., X-ray structure of ammonium perchlorate. II. Conventional refinement versus refinement with multipole deformation density functions, *Acta Cryst.*, **B35**, 1027 - 1033 (1976).

15. Becke, A.D., Density-functional thermochemistry. III. The role of exact exchange, *J. Chem. Phys.*, **98**, 5648 - 5652 (1993).

16. Lee, C.; Yang, W. and Parr, R.G., Development of the Colle-Salvetti correlation-energy formula into a functional of the electron density, *Phys. Rev. B.*, **37**, 785 - 789 (1988).

17. Miehlich, B.; Savin, A.; Stoll, H. and Preuss, H., Results obtained with the correlation energy density functionals of Becke and Lee, Yang and Parr, *Chem. Phys. Lett.*, **157**, 200-206 (1989).

18. Frisch, M.J.; Trucks, G.W.; Schlegel, H.B.; Scuseria, G.E.; Robb, M.A.; Cheeseman, J.R.; Zakrzewski, V.G.; Montgomery, J.A. Jr.; Stratmann, R.E.; Burant, J.C.; Dapprich, S.; Millam, J.M.; Daniels, A.D.; Kudin, K.N.; Strain, M.C.; Farkas, O.; Tomasi, J.; Barone, V.; Cossi, M.; Cammi, R.; Mennucci, B.; Pomelli, C.; Adamo, C.; Clifford, S.; Ochterski, J.; Petersson, G.A.; Ayala, P.Y.; Cui, Q.; Morokuma, K.; Malick, D.K.; Rabuck, A.D.; Raghavachari, K.; Foresman, J.B.; Cioslowski, J.; Ortiz, J.V.; Stefanov, B.B.; Liu, G.; Liashenko, A.; Piskorz, P.; Komaromi, I.; Gomperts, R.; Martin, R.L.; Fox, D.J.; Keith, T.; Al-Laham, M.A.; Peng, C.Y.; Nanayakkara, A.; Gonzalez, C.; Challacombe, M.; Gill, P.M.W.; Johnson, B.; Chen, W.; Wong, M.W.; Andres, J.L.; Gonzalez, C.; Head-Gordon, M.; Replogle, E.S. and Pople, J.A. (1998) *Gaussian 98, Rev. A.3*, Gaussian Inc., Pittsburgh PA.

19. Dorsett, H. and White, A., Overview of molecular modelling and ab initio molecular orbital methods suitable for use with energetic materials, DSTO General Document, DSTO-GD-0253 (2000).

20. Scott, A.P. and Radom, L., Harmonic vibrational frequencies: an evaluation of Hartree-Fock, Møller-Plesset, quadratic configuration interaction, density functional theory, and semiempirical scale factors, *J. Phys. Chem.*, **100**, 16502 - 16513 (1996).

21. Wong, M.W., Vibrational frequency prediction using density functional theory, *Chem. Phys. Lett.*, **256**, 391 - 399 (1996).

22. Bauschlicher, Jr., C.W. and Partridge, H., A modification of the Gaussian-2 approach using density functional theory, *J. Chem. Phys.*, **103**, 1788 - 1791 (1995).

23. Zhu, R.S. and Lin, M.C., Ab initio study of ammonium perchlorate combustion initiation processes: unimolecular decomposition of perchloric acid and the related OH + $ClO_3$ reaction, *PhysChemComm*, **25**, 1 - 6 (2001).

24. Salvador, P., Paizs, B., Duran, M. and Suhai, S., On the effect of the BSSE on intermolecular potential energy surfaces. Comparison of a priori and a posteriori BSSE correction schemes, *J. Comp. Chem.*, **22(7)**, 765 - 786 (2001).

# Appendix A: B3LYP/6-311+G(3df,2p) Molecular Pair Studies

Due to the failure of the B3LYP/6-31G(d) method to yield an activation energy for the transition state that was consistent with experimental data, calculations were performed using a larger basis set. Calculations were performed using a B3LYP method with a 6-311+G(3df,2p) basis set [15, 16, 17]. For energies of optimised structures, a zero-point energy correction was applied, with a scaling factor of 0.989 [22].

## A.1. Rocking between two equivalent initial structures

The initial structure obtained with the B3LYP/6-31G(d) basis set (Fig. 7a) was used as the starting structure for a geometry optimisation using the larger B3LYP/6-311+G(3df,2p) basis set. At this higher level, the symmetric structure shown for the initial structure above (Fig. 7a) is actually itself a transition state between two equivalent structures in which one N-H bond facing the perchlorate anion is longer than the other, similar to the transition state identified in Figure 7b, as shown in Figure 11.

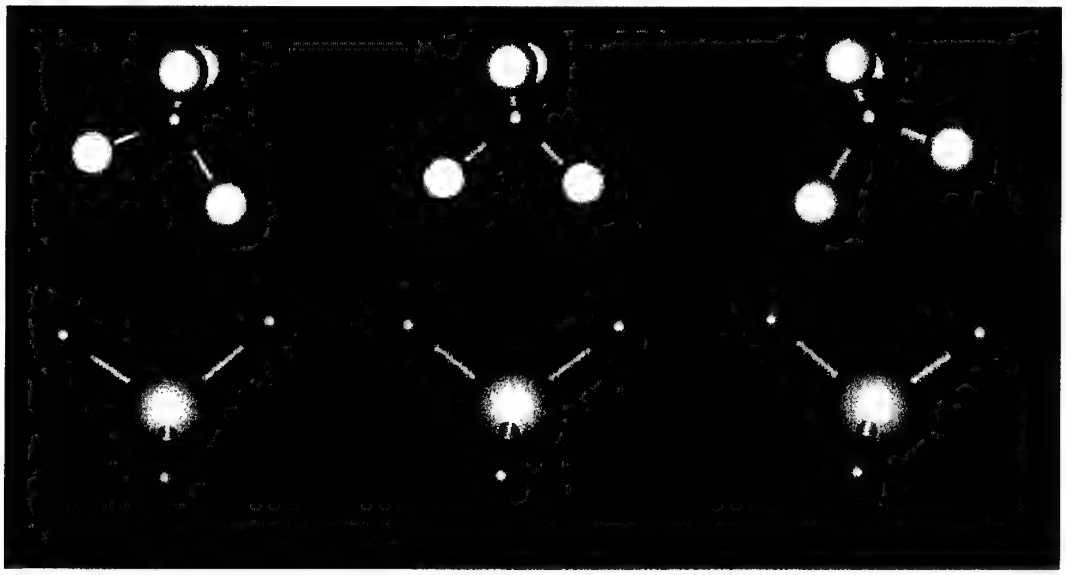

*Figure 11: Transition state structure (centre) for "rocking" between two equivalent initial state structures*

This may explain why the zero point corrected energy for the "transition state" above is actually lower in energy than those for the initial and final states – the transition state is actually the ground state for the $NH_4^+$ / $ClO_4^-$ system. Interatomic angles and distances are given in Tables 11 and 12 respectively, using the same atom numbering as before. The energies for these structures are given in Table 13. It can be seen that the

energy required to "rock" between the initial structures is very small, around 1.3 kJ/mol at 298.15 K.

*Table 11. Selected angles between three atoms ("bond angles") of the structures shown in Figure 11*

| Angle | Angle (°) | | |
|---|---|---|---|
| | Initial Structure | Transition State Structure | Initial' Structure |
| H9-O4-Cl1 | 109.6 | 112.3 | 114.9 |
| H8-O2-Cl1 | 114.9 | 113.0 | 109.6 |
| N6-H9-O4 | 168.5 | 147.6 | 120.1 |
| H8-N6-O4-Cl1 | -1.9 | -1.9 | 0.5 |
| H9-O4-Cl1-O2 | 1.5 | 3.9 | -0.7 |

*Table 12. Selected interatomic distances ("bond lengths") of the structures shown in Figure 11*

| distance | Interatomic Distance (Å) | | |
|---|---|---|---|
| | Initial Structure | Transition State Structure | Initial' Structure |
| H8-O2 | 2.10 | 1.70 | 1.41 |
| H9-O4 | 1.41 | 1.65 | 2.10 |
| N6-Cl1 | 3.26 | 3.21 | 3.26 |
| O2-Cl1 | 1.46 | 1.49 | 1.52 |
| O3-Cl1 | 1.43 | 1.43 | 1.43 |
| O4-Cl1 | 1.52 | 1.49 | 1.46 |
| O5-Cl1 | 1.43 | 1.43 | 1.43 |
| H7-N6 | 1.01 | 1.02 | 1.01 |
| H8-N6 | 1.02 | 1.05 | 1.13 |
| H9-N6 | 1.13 | 1.06 | 1.02 |
| H10-N6 | 1.01 | 1.02 | 1.01 |

*Table 13. B3LYP/6-311+G(3df,2p) energies of the new initial structure and the structure for the transition state between two equivalent initial structures as shown in Figure 11*

| Energy | Energy (au) | |
|---|---|---|
| | Initial structure | Structure for transition state for "rocking" between equivalent initial states (energy relative to Initial Structure (kJ/mol) |
| electronic energy | -818.146785 | -818.146416 (0.97) |
| zero point energy | 0.064164 | 0.065009 (2.22) |
| total energy at 0K | -818.082621 | -818.081407 (3.19) |
| total energy at 298.15K | -818.075354 | -818.074848 (1.33) |
| enthalpy | -818.074410 | -818.073904 (1.33) |
| free energy | -818.115277 | -818.113189 (5.48) |

## A.2. Proton transfer

A final structure after proton transfer (i.e., the $NH_3$ / $HClO_4$ system) at the B3LYP/6-311+G(3df,2p) level can be identified and appears similar to that shown for the lower level of theory above (Fig. 7c). Geometric parameters for this structure are given in Tables 14 and 15. The relevant energies are given in Table 16.

The relevant geometric parameters of the $NH_3/HClO_4$ complex are compared with those for $NH_3$ and $HClO_4$ in isolation in Table 17. The parameters for $HClO_4$ are essentially identical to those reported by Zhu and Lin [23] who studied the unimolecular decomposition of perchloric acid. This is to be expected as their calculations were also conducted at the B3LYP/6-311+G(3df,2p) level.

*Table 14. Selected angles between three atoms ("bond angles") for the B3LYP/6-311+G(3df, 2p) final structure after proton transfer ($NH_3$ / $HClO_4$)*

| Bond Angle | Angle (°) |
|---|---|
| H9-O4-Cl1 | 107.0 |
| H8-O2-Cl1 | 94.1 |
| N6-H9-O4 | 178.7 |
| H8-N6-O4-Cl1 | -42.3 |

*Table 15. Selected interatomic distances and angles ("bond lengths") for the B3LYP/6-311+G(3df, 2p) final structure after proton transfer ($NH_3$ / $HClO_4$)*

| Bond | Interatomic distance (Å) |
|---|---|
| O2-Cl1 | 1.43 |
| O3-Cl1 | 1.43 |
| O4-Cl1 | 1.60 |
| O5-Cl1 | 1.42 |
| H7-N6 | 1.02 |
| H8-N6 | 1.01 |
| H9-N6 | 1.58 |
| H10-N6 | 1.01 |
| H8-O2 | 3.14 |
| H9-O4 | 1.05 |
| N6-Cl1 | 3.44 |

The major difference in the geometric parameters of the complex compared to the isolated species are, as might be expected, in the H9-O4 and O4-Cl1 bond lengths of $HClO_4$. In the complex, the H9-O4 bond is longer and weaker as the hydrogen is drawn toward the $NH_3$ molecule and, as a consequence, the O4-Cl1 bond becomes stronger and shorter. Attempts to find a transition state for proton transfer between the initial structure for the $NH_4^+$ / $ClO_4^-$ system and the final structure (the $NH_3$ / $HClO_4$ system) at the B3LYP/6-311+G(3df,2p) level failed. Attempts using MP2/6-31G(d) and MP2/6-311G(d,p) also failed.

*Table 16. B3LYP/6-311+G(3df,2p) energies of the final structure*

| Energy | Energy (au) (energy relative to Initial Structure (kJ/mol) |
|---|---|
| electronic energy | -818.148537 (-4.6) |
| zero point energy | 0.063726 (-1.1) |
| total energy at 0K | -818.084812 (-5.7) |
| total energy at 298.15K | -818.077032 (-4.4) |
| enthalpy | -818.076087 (-4.4) |
| free energy | -818.119062 (-9.9) |

*Table 17. A comparison between geometric parameters for perchloric acid in the $NH_3/HClO_4$ complex described above with those obtained for perchloric acid in isolation. Both studies were conducted at the B3LYP/6-311+G(3df, 2p) level.*

| Bond Length (Å) | $NH_3/HClO_4$ complex | $NH_3$ or $HClO_4$ in isolation |
|---|---|---|
| O2-Cl1 | 1.43 | 1.42 |
| O3-Cl1 | 1.43 | 1.42 |
| O4-Cl1 | 1.60 | 1.66 |
| O5-Cl1 | 1.42 | 1.41 |
| H9-O4 | 1.05 | 0.97 |
| H7-N6 | 1.02 | 1.01 |
| H8-N6 | 1.01 | 1.01 |
| N10-N6 | 1.01 | 1.01 |
| Bond Angle (°) | | |
| H9-O4-Cl1 | 107.0 | 105.9 |
| O4-Cl1-O2 | 105.9 | 105.1 |
| O5-Cl1-O2 | 114.1 | 115.1 |
| H9-O4-Cl1-O5 | 177.2 | 179.7 |
| H9-O4-Cl1-O2 | 56.9 | 60.4 |
| H8-N6-H7 | 107.7 | 107.2 |
| H7-N6-H10 | 108.0 | 107.3 |
| H10-N6-H8 | 107.9 | 107.3 |
| H8-N6-H7-H10 | -116.3 | -115.0 |

DISTRIBUTION LIST

Ab Initio Computational Chemical Studies of Molecular Processes and Decomposition in Ammonium Perchlorate

A. White

**AUSTRALIA**

**DEFENCE ORGANISATION**

**Task Sponsor**

| | |
|---|---|
| Director – Ordnance Safety Group | 1 |

**S&T Program**

| | |
|---|---|
| Chief Defence Scientist<br>FAS Science Policy<br>AS Science Corporate Management<br>Director General Science Policy Development | shared copy |
| Counsellor Defence Science, London | Doc Data Sheet |
| Counsellor Defence Science, Washington | Doc Data Sheet |
| Scientific Adviser to MRDC, Thailand | Doc Data Sheet |
| Scientific Adviser Joint | 1 |
| Navy Scientific Adviser | Doc Data Sht & Dist List |
| Scientific Adviser - Army | 1 |
| Air Force Scientific Adviser | Doc Data Sht & Dist List |
| Scientific Adviser to the DMO M&A | Doc Data Sht & Dist List |
| Scientific Adviser to the DMO ELL | Doc Data Sht & Dist List |
| Director of Trials | 1 |

**Systems Sciences Laboratory**

| | |
|---|---|
| Chief of Weapons Systems Division | 1 |
| Research Leader – Emerging Weapon Technology | 1 |
| Head – Weapons Propulsion | 1 |
| Head – Explosives | 1 |
| Head – Pyrotechnics | 1 |
| Task Manager / Author: Dr Alex White | 10 |
| Dr Helen Dorsett (MOD) | 1 |

**DSTO Library and Archives**

| | |
|---|---|
| Library Edinburgh | 1 + Doc Data Sheet |
| Australian Archives | 1 |

**Capability Systems Division**

| | |
|---|---|
| Director General Maritime Development | Doc Data Sheet |
| Director General Land Development | 1 |
| Director General Aerospace Development | Doc Data Sheet |
| Director General Information Capability Development | Doc Data Sheet |

**Office of the Chief Information Officer**

| | |
|---|---|
| Deputy CIO | Doc Data Sheet |
| Director General Information Policy and Plans | Doc Data Sheet |
| AS Information Structures and Futures | Doc Data Sheet |
| AS Information Architecture and Management | Doc Data Sheet |
| Director General Australian Defence Simulation Office | Doc Data Sheet |

**Strategy Group**

| | |
|---|---|
| Director General Military Strategy | Doc Data Sheet |
| Director General Preparedness | Doc Data Sheet |

**HQAST**

| | |
|---|---|
| SO (Science) (ASJIC) | Doc Data Sheet |

**Navy**

| | |
|---|---|
| SO (SCIENCE), COMAUSNAVSURFGRP, NSW | Doc Data Sht & Dist List |
| Director General Navy Capability, Performance and Plans, Navy Headquarters | Doc Data Sheet |
| Director General Navy Strategic Policy and Futures, Navy Headquarters | Doc Data Sheet |

**Air Force**

| | |
|---|---|
| SO (Science) - Headquarters Air Combat Group, RAAF Base, Williamtown NSW 2314 | Doc Data Sht & Exec Summ |

**Army**

| | |
|---|---|
| ABCA National Standardisation Officer, Land Warfare Development Sector, Puckapunyal | e-mailed Doc Data Sheet |
| SO (Science), Deployable Joint Force Headquarters (DJFHQ) (L), Enoggera QLD | Doc Data Sheet |
| SO (Science) - Land Headquarters (LHQ), Victoria Barracks NSW | Doc Data & Exec Summ |

**Intelligence Program**

| | |
|---|---|
| DGSTA Defence Intelligence Organisation | 1 |
| Manager, Information Centre, Defence Intelligence Organisation | 1 (pdf version) |
| Assistant Secretary Corporate, Defence Imagery and Geospatial Organisation | Doc Data Sheet |

**Defence Materiel Organisation**

| | |
|---|---|
| Head Airborne Surveillance and Control | Doc Data Sheet |
| Head Aerospace Systems Division | Doc Data Sheet |
| Head Electronic Systems Division | Doc Data Sheet |
| Head Maritime Systems Division | Doc Data Sheet |
| Head Land Systems Division | Doc Data Sheet |
| Head Industry Division | Doc Data Sheet |
| Chief Joint Logistics Command | Doc Data Sheet |
| Management Information Systems Division | Doc Data Sheet |
| Head Materiel Finance | Doc Data Sheet |

**Defence Libraries**

| | |
|---|---|
| Library Manager, DLS-Canberra | Doc Data Sheet |
| Library Manager, DLS - Sydney West | Doc Data Sheet |

**OTHER ORGANISATIONS**

| | |
|---|---|
| National Library of Australia | 1 |
| NASA (Canberra) | 1 |

**UNIVERSITIES AND COLLEGES**

| | |
|---|---|
| Australian Defence Force Academy | |
| Library | 1 |
| Head of Aerospace and Mechanical Engineering | 1 |
| Serials Section (M list), Deakin University Library, Geelong, VIC | 1 |
| Hargrave Library, Monash University | Doc Data Sheet |
| Librarian, Flinders University | 1 |

**OUTSIDE AUSTRALIA**

**INTERNATIONAL DEFENCE INFORMATION CENTRES**

| | |
|---|---|
| US Defense Technical Information Center | 2 |
| UK Defence Research Information Centre | 2 |
| Canada Defence Scientific Information Service | e-mail link to pdf |
| NZ Defence Information Centre | 1 |

**ABSTRACTING AND INFORMATION ORGANISATIONS**

| | |
|---|---|
| Library, Chemical Abstracts Reference Service | 1 |
| Engineering Societies Library, US | 1 |
| Materials Information, Cambridge Scientific Abstracts, US | 1 |
| Documents Librarian, The Center for Research Libraries, US | 1 |

| | |
|---|---|
| SPARES | 5 |

**Total number of copies:** **44 printed** **2 pdf** **46**

*This page intentionally left blank*

**DEFENCE SCIENCE AND TECHNOLOGY ORGANISATION**
**DOCUMENT CONTROL DATA**

1. PRIVACY MARKING/CAVEAT (OF DOCUMENT)

2. TITLE

Ab Initio Computational Chemical Studies of Molecular Processes and Decomposition in Ammonium Perchlorate

3. SECURITY CLASSIFICATION (FOR UNCLASSIFIED REPORTS THAT ARE LIMITED RELEASE USE (L) NEXT TO DOCUMENT CLASSIFICATION)

| | |
|---|---|
| Document | (U) |
| Title | (U) |
| Abstract | (U) |

4. AUTHOR(S)

A. White

5. CORPORATE AUTHOR

Systems Sciences Laboratory
PO Box 1500
Edinburgh South Australia 5111 Australia

| 6a. DSTO NUMBER | 6b. AR NUMBER | 6c. TYPE OF REPORT | 7. DOCUMENT DATE |
|---|---|---|---|
| DSTO-TR-1552 | AR-013-032 | Technical Report | February 2004 |

| 8. FILE NUMBER | 9. TASK NUMBER | 10. TASK SPONSOR | 11. NO. OF PAGES | 12. NO. OF REFERENCES |
|---|---|---|---|---|
| E9505/23/109/1 | JTW 03/066 | DOSG | 26 | 24 |

13. URL on the World Web

http://www.dsto.defence.gov.au/corporate/reports/DSTO-TR-1552.pdf

14. RELEASE AUTHORITY

Chief, Weapons Systems Division

15. SECONDARY RELEASE STATEMENT OF THIS DOCUMENT

*Approved for public release*

OVERSEAS ENQUIRIES OUTSIDE STATED LIMITATIONS SHOULD BE REFERRED THROUGH DOCUMENT EXCHANGE, PO BOX 1500, EDINBURGH, SA 5111

16. DELIBERATE ANNOUNCEMENT

No Limitations

17. CITATION IN OTHER DOCUMENTS Yes

18. DEFTEST DESCRIPTORS

ammonium perchlorate, decomposition reactions, oxidizers, computational chemistry, energetic materials, quantum theory, molecular modelling

19. ABSTRACT

Ammonium perchlorate is widely used as an oxidiser in composite propellants for rocket motors. Its decomposition is of interest in stability, sensitivity and combustion studies for rocket motor safety and performance analysis and prediction. This document presents some theoretical studies conducted to yield insights into the mechanisms and kinetics of ammonium perchlorate decomposition.

*This page intentionally left blank*